Frustrated FRET for high-contrast high-resolution two-photon imaging

Fang Xu, Lu Wei, Zhixing Chen, and Wei Min*

Department of Chemistry, Columbia University, New York, New York 10027, USA
*wm2256@columbia.edu

Abstract: Two-photon fluorescence microscopy has become increasingly popular in biomedical research as it allows high-resolution imaging of thick biological specimen with superior contrast and penetration than confocal microscopy. However, two-photon microscopy still faces two fundamental limitations: 1) image-contrast deterioration with imaging depth due to out-of-focus background and 2) diffraction-limited spatial resolution. Herein we propose to create and detect high-order (more than quadratic) nonlinear signals by harnessing the frustrated fluorescence resonance energy transfer (FRET) effect within a specially designed donor-acceptor probe pair. Two distinct techniques are described. In the first method, donor fluorescence generated by a two-photon laser at the focus is preferentially switched on and off by a modulated and focused one-photon laser beam that is able to block FRET via direct acceptor excitation. The resulting image, constructed from the enhanced donor fluorescence signal, turns out to be an overall three-photon process. In the second method, a two-photon laser at a proper wavelength is capable of simultaneously exciting both the donor and the acceptor. By sinusoidally modulating the two-photon excitation laser at a fundamental frequency ω, an overall four-photon signal can be isolated by demodulating the donor fluorescence at the third harmonic frequency 3ω. We show that both the image contrast and the spatial resolution of the standard two-photon fluorescence microscopy can be substantially improved by virtue of the high-order nonlinearity. This frustrated FRET approach represents a strategy that is based on extracting the inherent nonlinear photophysical response of the specially designed imaging probes.

OCIS codes: (170.2520) Fluorescence microscopy; (170.4090) Modulation techniques; (170.5810) Scanning microscopy; (180.4315) Nonlinear microscopy; (190.4180) Multiphoton processes; (290.0290) Scattering.

References and links

1. R. Yuste, ed., *Imaging: A Laboratory Manual* (Cold Spring Harbor Laboratory, 2010).
2. W. Denk, J. H. Strickler, and W. W. Webb, "Two-photon laser scanning fluorescence microscopy," Science **248**(4951), 73–76 (1990).
3. F. Helmchen and W. Denk, "Deep tissue two-photon microscopy," Nat. Methods **2**(12), 932–940 (2005).
4. B. R. Master and P. T. C. So, *Handbook of Biomedical Nonlinear Optical Microscopy* (Oxford University, 2008).
5. P. Theer and W. Denk, "On the fundamental imaging-depth limit in two-photon microscopy," J. Opt. Soc. Am. A **23**(12), 3139–3149 (2006).
6. P. Theer, M. T. Hasan, and W. Denk, "Two-photon imaging to a depth of 1000 μm in living brains by use of a Ti:Al_2O_3 regenerative amplifier," Opt. Lett. **28**(12), 1022–1024 (2003).
7. J. Ying, F. Liu, and R. R. Alfano, "Spatial distribution of two-photon-excited fluorescence in scattering media," Appl. Opt. **38**(1), 224–229 (1999).
8. N. J. Durr, C. T. Weisspfennig, B. A. Holfeld, and A. Ben-Yakar, "Maximum imaging depth of two-photon autofluorescence microscopy in epithelial tissues," J. Biomed. Opt. **16**(2), 026008 (2011).
9. D. Kobat, N. G. Horton, and C. Xu, "In vivo two-photon microscopy to 1.6-mm depth in mouse cortex," J. Biomed. Opt. **16**(10), 106014 (2011).

#185684 - $15.00 USD Received 20 Feb 2013; revised 1 Apr 2013; accepted 2 Apr 2013; published 5 Jun 2013

10. N. Ji, D. E. Milkie, and E. Betzig, "Adaptive optics via pupil segmentation for high-resolution imaging in biological tissues," Nat. Methods **7**(2), 141–147 (2010).
11. M. Rueckel, J. A. Mack-Bucher, and W. Denk, "Adaptive wavefront correction in two-photon microscopy using coherence-gated wavefront sensing," Proc. Natl. Acad. Sci. U.S.A. **103**(46), 17137–17142 (2006).
12. A. Leray, K. Lillis, and J. Mertz, "Enhanced background rejection in thick tissue with differential-aberration two-photon microscopy," Biophys. J. **94**(4), 1449–1458 (2008).
13. M. A. A. Neil, R. Juskaitis, and T. Wilson, "Method of obtaining optical sectioning by using structured light in a conventional microscope," Opt. Lett. **22**(24), 1905–1907 (1997).
14. Z. Yaqoob, D. Psaltis, M. S. Feld, and C. Yang, "Optical phase conjugation for turbidity suppression in biological samples," Nat. Photonics **2**(2), 110–115 (2008).
15. G. Zhu, J. van Howe, M. Durst, W. Zipfel, and C. Xu, *Simultaneous Spatial and Temporal Focusing of Femtosecond Pulses* (Conference on Lasers and Electro-Optics (CLEO), 2005).
16. N. Chen, C. H. Wong, and C. J. Sheppard, "Focal modulation microscopy," Opt. Express **16**(23), 18764–18769 (2008).
17. J. B. Ding, K. T. Takasaki, and B. L. Sabatini, "Supraresolution imaging in brain slices using stimulated-emission depletion two-photon laser scanning microscopy," Neuron **63**(4), 429–437 (2009).
18. P. Bianchini, B. Harke, S. Galiani, G. Vicidomini, and A. Diaspro, "Single-wavelength two-photon excitation-stimulated emission depletion (SW2PE-STED) superresolution imaging," Proc. Natl. Acad. Sci. U.S.A. **109**(17), 6390–6393 (2012).
19. E. Betzig, G. H. Patterson, R. Sougrat, O. W. Lindwasser, S. Olenych, J. S. Bonifacino, M. W. Davidson, J. Lippincott-Schwartz, and H. F. Hess, "Imaging intracellular fluorescent proteins at nanometer resolution," Science **313**(5793), 1642–1645 (2006).
20. M. J. Rust, M. Bates, and X. Zhuang, "Sub-diffraction-limit imaging by stochastic optical reconstruction microscopy (STORM)," Nat. Methods **3**(10), 793–796 (2006).
21. M. G. L. Gustafsson, "Nonlinear structured-illumination microscopy: wide-field fluorescence imaging with theoretically unlimited resolution," Proc. Natl. Acad. Sci. U.S.A. **102**(37), 13081–13086 (2005).
22. T. Dertinger, R. Colyer, G. Iyer, S. Weiss, and J. Enderlein, "Fast, background-free, 3D super-resolution optical fluctuation imaging (SOFI)," Proc. Natl. Acad. Sci. U.S.A. **106**(52), 22287–22292 (2009).
23. S. W. Hell and J. Wichmann, "Breaking the diffraction resolution limit by stimulated emission: stimulated-emission-depletion fluorescence microscopy," Opt. Lett. **19**(11), 780–782 (1994).
24. S. Berning, K. I. Willig, H. Steffens, P. Dibaj, and S. W. Hell, "Nanoscopy in a living mouse brain," Science **335**(6068), 551 (2012).
25. M. Beutler, K. Makrogianneli, R. J. Vermeij, M. Keppler, T. Ng, T. M. Jovin, and R. Heintzmann, "satFRET: estimation of Forster resonance energy transfer by acceptor saturation," Eur. Biophys. J. **38**(1), 69–82 (2008).
26. P. E. Hänninen, L. Lehtelä, and S. W. Hell, "Two- and multiphoton excitation of conjugate-dyes using a continuous wave laser," Opt. Commun. **130**(1-3), 29–33 (1996).
27. A. Schönle, P. E. Hanninen, and S. W. Hell, "Nonlinear fluorescence through intermolecular energy transfer and resolution increase in fluorescence microscopy," Ann. Phys. **8**(2), 115–133 (1999).
28. C. I. Richards, J. C. Hsiang, A. M. Khalil, N. P. Hull, and R. M. Dickson, "FRET-enabled optical modulation for high sensitivity fluorescence imaging," J. Am. Chem. Soc. **132**(18), 6318–6323 (2010).
29. K. Fujita, M. Kobayashi, S. Kawano, M. Yamanaka, and S. Kawata, "High-resolution confocal microscopy by saturated excitation of fluorescence," Phys. Rev. Lett. **99**(22), 228105 (2007).
30. J. Lukomska, I. Gryczynski, J. Malicka, S. Makowiec, J. R. Lakowicz, and Z. Gryczynski, "Two-photon induced fluorescence of Cy5-DNA in buffer solution and on silver island films," Biochem. Biophys. Res. Commun. **328**(1), 78–84 (2005).
31. W. R. Zipfel, R. M. Williams, and W. W. Webb, "Nonlinear magic: multiphoton microscopy in the biosciences," Nat. Biotechnol. **21**(11), 1369–1377 (2003).
32. Y.-T. Kao, X. Zhu, F. Xu, and W. Min, "Focal switching of photochromic fluorescent proteins enables multiphoton microscopy with superior image contrast," Biomed. Opt. Express **3**(8), 1955–1963 (2012).
33. Z. Chen, L. Wei, X. Zhu, and W. Min, "Extending the fundamental imaging-depth limit of multi-photon microscopy by imaging with photo-activatable fluorophores," Opt. Express **20**(17), 18525–18536 (2012).
34. X. Zhu, Y.-T. Kao, and W. Min, "Molecular-switch-mediated multiphoton fluorescence microscopy with high-order nonlinearity," J. Phys. Chem. Lett. **3**(15), 2082–2086 (2012).

1. Introduction

Modern optical microscopy has greatly opened up exciting opportunities for imaging biological samples. For high-resolution (sub-cellular) imaging in live tissues and organisms, two-photon (2P) fluorescence microscopy is the most appealing tool [1–3]. It uses localized nonlinear excitation to generate fluorescence signal within the focus volume where the probability of absorbing two simultaneous incident photons in a single event is the highest [4]. In comparison to one-photon confocal microscopy, such spatially confined excitation

#185684 - $15.00 USD Received 20 Feb 2013; revised 1 Apr 2013; accepted 2 Apr 2013; published 5 Jun 2013

(i.e., optical sectioning) of 2P microscopy enables higher image contrast and hence deeper penetration for scattering samples.

However, 2P microscopy will finally lose its image contrast when the optical sectioning ability eventually breaks down when focusing deep into scattering samples. Due to the scattering loss, the laser power is attenuated exponentially along the light path. Increasing the total excitation laser power with imaging depth helps to maintain the same excitation intensity at the focal plane, but inevitably also raises the probability of exciting the out-of-focus fluorophores (especially those located near the sample surface). As a result, the out-of-focus background will grow and eventually overwhelm the in-focal signal when approaching the fundamental imaging-depth limit [5–8]. Obviously, such loss of image contrast cannot be overcome with a higher excitation laser power which will enhance the signal and background equally. A number of strategies have been devised to address this challenge, including using longer excitation wavelength [9], adaptive optics [10, 11], differential aberration [12], structured illumination [13], optical phase conjugation [14], spatial and temporal focusing [15] and focal modulation [16].

In addition to the loss of image contrast, 2P microscopy also suffers from relatively coarse diffraction-limited spatial resolution [17, 18]. Due to the long excitation wavelength and moderate numerical aperture of the objective, the lateral resolution of 2P microscopy is only about 400 nm which obscures many interesting features such as dendritic spines. Although several super-resolution techniques (PALM [19], STORM [20], SIM [21], SOFI [22] and STED [23]) have been developed to break the diffraction limit, only STED [17, 23, 24] is compatible with 2P imaging because STED is equipped with single-element detectors rather than CCD cameras. Unfortunately, it is technically challenging for two-photon STED to spatially shape a doughnut beam with clean intensity null deep inside highly scattering samples.

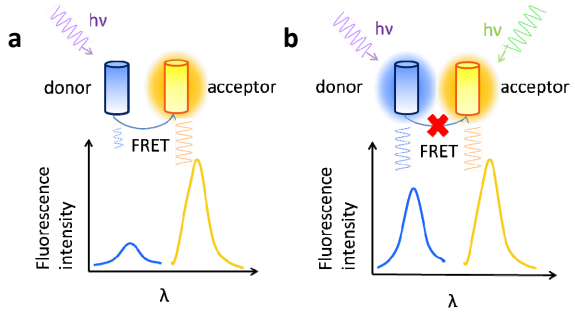

Fig. 1. Principle of frustrated FRET. (a) When only the donor is excited, the fluorescence resonance energy is transferred from the donor to the acceptor, quenching the donor fluorescence. (b) When the donor and the acceptor are excited at the same time, FRET is inhibited, recovering the donor fluorescence.

Herein we propose a new concept of harnessing higher-order (more than quadratic) nonlinear fluorescence to improve both the spatial resolution and image contrast of 2P microscopy. Instead of involving more virtual states, the super nonlinearity is created by frustrated FRET, i.e., blocking energy transfer from the donor to the acceptor in a FRET pair. In brief, if the donor alone is excited, FRET will occur between the excited donor and the ground state acceptor, which quenches the donor fluorescence. In contrast, if the donor and the acceptor are both excited, energy transfer will be largely blocked (due to the mismatch of spectral overlap) and thus the donor fluorescence will be dequenched and enhanced [Fig. 1] [25]. Therefore, frustrated FRET is inherently a nonlinear process requiring excitation of both donor and acceptor. The concept of frustrated FRET was originally proposed to enhance the resolution of confocal microscopy [26, 27], and was recently applied in selective synchronously amplified fluorescence image recovery from a high background [28]. Here we

#185684 - $15.00 USD Received 20 Feb 2013; revised 1 Apr 2013; accepted 2 Apr 2013; published 5 Jun 2013

exploit it for enhancing image contrast and the spatial resolution of 2P microscopy in scattering samples.

In this report, we propose two distinct but related experimental schemes to generate and detect such super-nonlinearity associated with frustrated FRET. The first technique utilizes a modulated one-photon (1P) laser beam to directly excite the acceptor, preferentially switching on/off the FRET process. The enhanced donor fluorescence is proved to be an overall three-photon process. The second technique employs only one 2P laser that could excite both the donor and acceptor. The 2P laser is modulated at a fundamental frequency ω and an overall four-photon donor fluorescence signal is deciphered at the third harmonic frequency 3ω through demodulation [29]. We present the expected performance of both new 2P imaging techniques with analytical theory and numerical simulations.

2. Results and discussion

2.1 Frustrated FRET implemented with two excitation beams

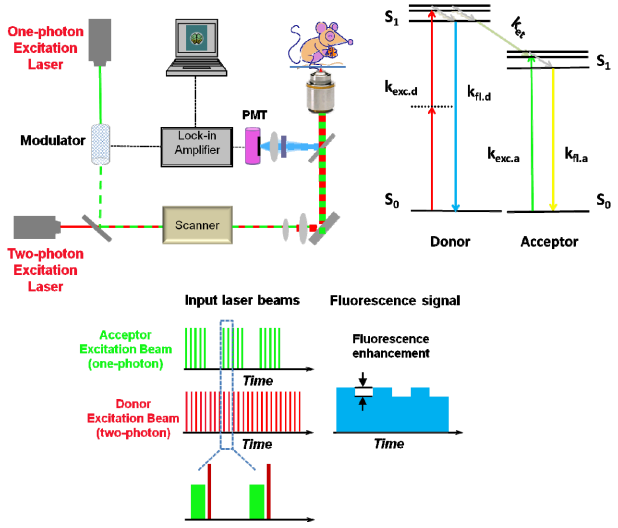

Fig. 2. Frustrated FRET with two excitation beams. (a) The proposed experimental setup in which the 2P laser and the 1P laser are collinearly combined with each other and focused onto the same focal spot. The 1P laser beam is being modulated, and the demodulated donor fluorescence is used as the new signal contrast. (b) A simplified Joblonski diagram illustrating that the energy is blocked by simultaneous excitation of both the donor and the acceptor. (c) Synchronized donor/acceptor excitation pulse trains. The 1P laser pulses are temporally followed by the 2P laser pulses with a time gap shorter than 1ns, which avoids the potential stimulated emission of the donor but still blocks FRET efficiently. The final image is reconstructed from the enhanced fluorescence signal which is demodulated from the lock-in amplifier.

In the first approach, as shown in Fig. 2(a), a two-photon (2P) laser for donor excitation is collinearly combined with a one-photon (1P) laser beam for direct acceptor excitation. Both 2P and 1P excitation beams are pulsed lasers (synchronized at the same frequency ~80MHz) with pulse widths of ~100fs and ~1ns, respectively. As the fluorescence lifetime (~3ns) is much shorter than the pulse spacing (~13ns), the donor and the acceptor are treated on their ground states right before each pulses. Note that to avoid the potential donor stimulated emission caused by the 1P excitation beam, the 1P pulse train is temporally ahead of the 2P train for each pulse by sub-nanoseconds [Fig. 2(c)]. The 1P laser is intensity modulated at a high frequency (~5MHz). When the 1P laser is blocked, an efficient FRET occurs from the 2P-excited donor to the ground state acceptor, resulting in a low donor fluorescence signal. In contrast, when 1P laser is unblocked, the acceptor will be brought to the excited state right

#185684 - $15.00 USD Received 20 Feb 2013; revised 1 Apr 2013; accepted 2 Apr 2013; published 5 Jun 2013

before the action of 2P pulses, which inhibits FRET process and enhances the donor fluorescence. The final image is thus reconstructed from the enhanced donor fluorescence signal detected by a lock-in amplifier at the modulation frequency. In principle, all regular FRET pairs can work for this technique. In practice, we prefer donors to have high 2P absorption cross-section and high quantum yield. Besides a fluorophore, the acceptor could also be a non-fluorescent quencher. Fluorophores or quenchers with red-shifted excitation spectra are preferred as the FRET acceptors, in which case the wavelength of the 1P acceptor excitation laser (λ_{1P}) will be close to that of the 2P donor excitation laser (λ_{2P}), ensuring similar attenuation effects.

Quantitatively, under illumination by a train of 2P laser pulses, the excitation rate constant of the donor within the short laser pulses is related to I_{2P} through

$$k_{exc,d} = \sigma_{d,2P}\left(\frac{I_{2P,ave}\lambda_{2P}}{f_{rep}\delta_{2P}hc}\right)^2. \quad (1)$$

Similarly, the excitation rate constant of the acceptor within the 1P laser pulse is related to I_{1P} through

$$k_{exc,a} = \sigma_{a,1P}\left(\frac{I_{1P,ave}\lambda_{1P}}{f_{rep}\delta_{1P}hc}\right). \quad (2)$$

where $\sigma_{d,2P}$ is the two-photon absorption cross section (GM) of the donor at wavelength λ_{2P}, $\sigma_{a,1P}$ is the one-photon absorption cross section (cm^2) of the acceptor at wavelength λ_{1P}, f_{rep} is the repetition rate (~80 MHz), δ_{2P} is 2P pulse width (~100 fs) and δ_{1P} is 1P pulse width (~1 ns).

The probability of the donor or the acceptor being excited to the excited state after each laser pulse is determined by the first-order kinetics $P = 1-\exp(-k_{exc}\delta_{pulse})$. Note that there will be negligible excited-state molecules decaying back to the ground state within the short pulse duration. Under the non-saturating condition, the probability simplifies to $P \approx k_{exc}\delta_{pulse}$. Because the excitation of the donor and the acceptor are independent processes, after each pulse, the probabilities of the donor and the acceptor being excited to the excited states are

$$P_D = \sigma_{d,2P}\delta_{2P}\left(\frac{I_{2P,ave}\lambda_{2P}}{f_{rep}\delta_{2P}hc}\right)^2, \quad (3)$$

and

$$P_A = \sigma_{a,1P}\delta_{1P}\left(\frac{I_{1P,ave}\lambda_{1P}}{f_{rep}\delta_{1P}hc}\right). \quad (4)$$

When the 1P acceptor excitation laser is blocked (off) during the modulation procedure, energy will be transferred between the excited donor and ground state acceptor, quenching the donor fluorescence. The donor fluorescent emission rate in the absence of 1P excitation beam is

$$S_{fl,d} = N\varepsilon f_{rep}P_D\frac{k_{fl,d}}{k_{fl,d}+k_{FRET}} = N\varepsilon f_{rep}P_D\frac{1/\tau}{1/\tau+k_{FRET}}, \quad (5)$$

#185684 - $15.00 USD Received 20 Feb 2013; revised 1 Apr 2013; accepted 2 Apr 2013; published 5 Jun 2013

where N is the number of fluorophores, ε is the collection efficiency, $k_{fl,d}$ is the fluorescence emission rate of the donor, τ is the intrinsic donor fluorescence lifetime, and k_{FRET} is the energy transfer rate. We have assumed the original donor fluorescence quantum yield as unity.

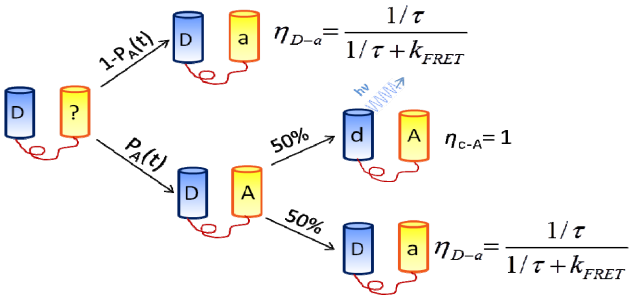

Fig. 3. Several possible fates of the P_D (t) population are considered when the 1P acceptor excitation beam is on. The capital letters denote the excited states of the donor (D) and acceptor (A), and the small letters denote the ground states of the donor (d) and the acceptor (a).

We then consider the case when the 1P acceptor excitation beam is on. As schematized in Fig. 3, the donor fluorescence quantum yield is determined with two possible scenarios after each pulse: the acceptor remains in the ground state, which has a probability of $1-P_A$, and the acceptor is also excited to the excited state, which has a probability of P_A. For the first scenario, the donor fluorescence quantum yield for such a D-a pair is the same as that in Eq. (5), i.e., $(1/\tau)/\left[(1/\tau)+k_{FRET}\right]$. For the second scenario of the excited D-A pair, if assuming comparable fluorescence lifetimes for the donor and the acceptor, there exist two sub-scenarios with certain chances (we assume the chance to be 50:50). If the acceptor is relaxed to the ground state earlier than the donor, the donor fluorescence quantum yield is given by Eq. (5) as well. On the other hand, if the acceptor is relaxed to the ground state later than the donor, the donor fluorescence quantum yield is then 1. Therefore, we can calculate the weighted donor fluorescence quantum yield for P_D population as:

$$\begin{aligned}\eta' &= [1-P_A]\cdot\frac{1/\tau}{1/\tau+k_{FRET}} + P_A\cdot\left(\frac{1}{2}+\frac{1}{2}\cdot\frac{1/\tau}{1/\tau+k_{FRET}}\right)\\ &= \frac{1/\tau}{1/\tau+k_{FRET}} + \frac{1}{2}P_A\cdot\frac{k_{FRET}}{1/\tau+k_{FRET}},\end{aligned} \tag{6}$$

where $k_{FRET}/\left[(1/\tau)+k_{FRET}\right]$ is the energy transfer efficiency E_t. The detected donor fluorescence emission rate S_{fl}' in the presence of 1P beam thus becomes:

$$S_{fl,d}' = N\varepsilon f_{rep}P_D\eta' = N\varepsilon f_{rep}P_D\left(\frac{1/\tau}{1/\tau+k_{FRET}} + \frac{1}{2}P_A E_t\right). \tag{7}$$

Subtracting Eq. (5) from Eq. (7) which is equivalent to the electronic demodulation of the lock-in amplifier at the modulation frequency [Fig. 2(c)], we finally arrive at the enhanced donor fluorescent signal:

$$S_{enhanced} = \frac{1}{2}N\varepsilon f_{rep}E_t P_D P_A = \alpha I_{2P,ave}{}^2 I_{1P,ave}, \tag{8}$$

#185684 - $15.00 USD Received 20 Feb 2013; revised 1 Apr 2013; accepted 2 Apr 2013; published 5 Jun 2013

where $\alpha = 1/2N\,\varepsilon f_{rep} E_t \left[\delta_{2P}\sigma_{d,2P}\left(\lambda_{2P}/f_{rep}\delta_{2P}hc\right)^2\right]\left[\delta_{1P}\sigma_{a,1P}\left(\lambda_{1P}/f_{rep}\delta_{1P}hc\right)\right]$. The original two-photon process has now been turned into an overall three-photon effect after harnessing the frustrated FRET effect. It is worth noting that the FRET efficiency (E_t) does not affect the super-nonlinearity generated by frustrated FRET. On the other hand, the detected fluorescence signal depends on E_t, thus the FRET pairs with high energy transfer efficiencies are desired to achieve high photon flux.

2.2 Frustrated FRET implemented with one excitation beam

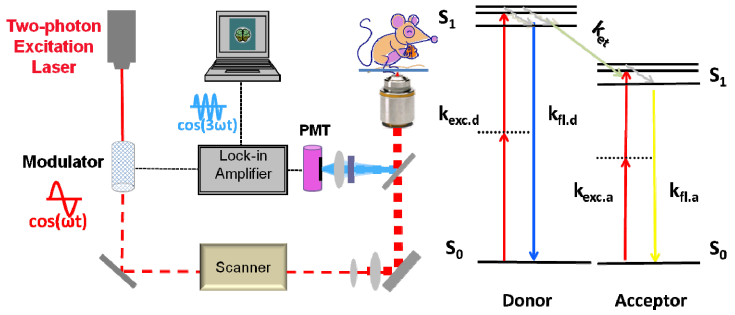

Fig. 4. Frustrated FRET with one excitation beam (a) The proposed experimental setup in which the 2P laser is sinusoidally modulated at the fundamental frequency ω, and the donor fluorescence detected and then demodulated at 3ω. (b) A simplified Joblonski diagram illustrating that the energy transfer is blocked by simultaneous excitation of both the donor and the acceptor with a two-photon laser.

Now we utilize only one 2P laser beam at a proper wavelength that can excite both the donor and the acceptor. It should be easy to design such FRET pairs, as two-photon absorption spectra of most dyes are rather broad. For example, Rhodamine B and Cy5 are promising donor and acceptor candidates, because of the high 2P excitation efficiency at 820~840 nm, bright donor fluorescence and small emission overlap [30]. By sinusoidally modulating the excitation 2P laser at a fundamental frequency (ω) and demodulating the donor fluorescence at the third harmonic frequency (3ω), the higher-order nonlinear signal could be isolated. Thus, a relatively simple apparatus can realize this harmonic demodulation concept [Fig. 4(a)].

Upon intensity modulation at fundamental frequency ω (~MHz, which is fast enough for point scanning but slower than the pulse repetition), the average 2P excitation intensity could be sinusoidally modulated as:

$$I_{2P,ave}(t) = \left\langle I_{2P,ave}\right\rangle\left[1+\alpha\cos(\omega t)\right], \tag{9}$$

where $\left\langle I_{2P,ave}\right\rangle$ is the time-averaged value of $I_{2P,ave}(t)$, and α is the modulation depth (here we assume α = 1). During each pulse, the excitation rate constant within the short laser pulses is defined as

$$k_{exc,2P}(t) = \sigma_{2P}{}'\left(\frac{I_{2P,ave}(t)\lambda_{2P}{}'}{f_{rep}\delta_{pulse}hc}\right)^2. \tag{10}$$

The modulated probability of the donor or the acceptor being excited to the excited state after each laser pulse is $P(t) \approx k_{exc,2P}(t)\delta_{pulse}$. After each pulse, the probability of the donor and the acceptor being excited to the excited states are

#185684 - $15.00 USD Received 20 Feb 2013; revised 1 Apr 2013; accepted 2 Apr 2013; published 5 Jun 2013

$$P_D(t) = \beta_D \left[1 + \cos \omega t\right]^2, \tag{11}$$

and

$$P_A(t) = \beta_A \left[1 + \cos \omega t\right]^2, \tag{12}$$

where $\beta_{A,D} \equiv \sigma_{A,D} \delta_{pulse} \left(\lambda_{2P} \left\langle I_{2P,ave} \right\rangle / f_{rep} \delta_{pulse} hc \right)^2$, representing the time-averaged excitation probability of a single acceptor or donor.

Then we determine the fluorescence quantum yield for the $P_D(t)$ donor population. As described in the previous section [Fig. 3], there are two possible scenarios facing this population of $P_D(t)$ after each pulse as well. The resulting modulated quantum yield of the donor fluorescence is presented as

$$\eta(t) = \frac{1/\tau}{1/\tau + k_{FRET}} + \frac{1}{2} P_A(t) E_t. \tag{13}$$

Thus the detected fluorescence emission rate $S_{fl}(t)$ of the donor is

$$S_{fl}(t) = N \varepsilon f_{rep} P_D(t) \eta(t). \tag{14}$$

Incorporating Eqs. (11)-(13) into Eq. (14), we arrive at:

$$S_{fl,d}(t) = N \varepsilon f_{rep} \beta_D \frac{1/\tau}{1/\tau + k_{FRET}} \left[1 + \cos(\omega t)\right]^2 + \frac{1}{2} N \varepsilon f_{rep} E_t \beta_D \beta_A \left[1 + \cos(\omega t)\right]^4. \tag{15}$$

As expected, the donor fluorescent signal consists of both a quadratic term and a quartic term.

Harmonic demodulation technique is then employed to separate the quartic term from Eq. (15): modulating the 2P laser beam at a fundamental frequency ω and then demodulating the detected fluorescence signal at 3ω. Quantitatively, we expand Eq. (15) into its Fourier series:

$$S_{fl,d}(t) = (N \varepsilon f_{rep}) \left[S_0 + S_\omega \cos(\omega t) + S_{2\omega} \cos(2\omega t) + S_{3\omega} \cos(3\omega t) + S_{4\omega} \cos(4\omega t)\right], \tag{16}$$

where the Fourier coefficients $S_{n\omega}$ represent the amplitude of the *n*th harmonic frequency, and have forms as:

$$S_0 = \frac{3}{2} \frac{1/\tau}{1/\tau + k_{FRET}} \beta_D + \frac{25}{16} E_t \beta_D \beta_A, \tag{17}$$

$$S_\omega = \frac{1}{2} \frac{1/\tau}{1/\tau + k_{FRET}} \beta_D + \frac{3}{2} E_t \beta_D \beta_A, \tag{18}$$

$$S_{2\omega} = 2 \frac{1/\tau}{1/\tau + k_{FRET}} \beta_D + \frac{5}{2} E_t \beta_D \beta_A, \tag{19}$$

$$S_{3\omega} = \frac{1}{2} E_t \beta_D \beta_A, \tag{20}$$

$$S_{4\omega} = \frac{1}{16} E_t \beta_D \beta_A. \tag{21}$$

Assuming that $\beta_A = \beta_D = \beta$, we obtain the dependence of demodulated donor fluorescent signal at the frequencies of ω, 2ω, 3ω, and 4ω as functions of β. As shown in Fig. 5, the 3ω

#185684 - $15.00 USD Received 20 Feb 2013; revised 1 Apr 2013; accepted 2 Apr 2013; published 5 Jun 2013

and 4ω harmonic signals scale with β^2 only, while the ω, 2ω signals contain a mixture of β and β^2 terms. Since β is given by $\sigma\delta_{pulse}\left(\lambda_{2P}\left\langle I_{2P,ave}\right\rangle / f_{rep}\delta_{pulse}hc\right)^2$, thus purely four-photon signals can be detected at the 3ω and 4ω harmonic frequencies. Furthermore, if assuming E_t as 80%, a common energy transfer efficiency value between FRET pairs, we will get $S_{3\omega}/S_0 = \beta/(0.75+3.125\beta)$. If a moderate excitation probability (β = 0.1) is assumed, the 3ω harmonic fluorescent signal is about 9.4% of the regular 2P signal. Therefore, a sizable four-photon fluorescent signal can be detected at the 3ω demodulated harmonic frequency.

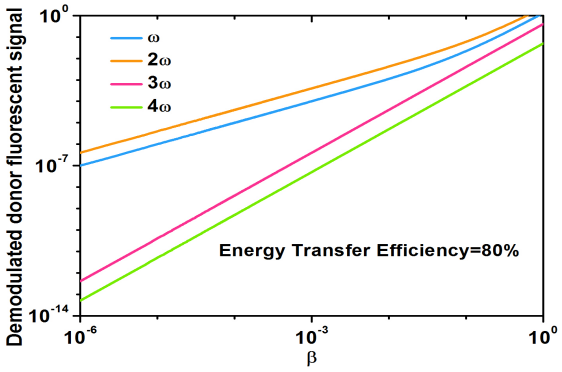

Fig. 5. Dependence of demodulated donor fluorescence (after normalization) at ω (S_ω), 2ω ($S_{2\omega}$), 3ω ($S_{3\omega}$) and 4ω ($S_{4\omega}$) as a function of β in the one-laser scheme. Note that β itself scales with $\left\langle I_{2p,ave}\right\rangle^2$. Thus under non-saturating condition, 3ω and 4ω harmonic demodulation signals scale with $\left\langle I_{2p,ave}\right\rangle^4$.

2.3 Enhancement of signal-to-background contrast deep inside scattering samples

Now we numerically estimate how the above two new frustrated FRET techniques could enhance the signal-to-background contrast at fundamental imaging-depth limit of the regular two-photon microscopy, which is defined as [5–8]

$$\left(\frac{S}{B}\right)_{2P} = \frac{\int_{V_{in}}\int_0^\tau C_s(r,z)I_{2P}{}^2(r,z,t)dtdV}{\int_{V_{out}}\int_0^\tau C_B(r,z)I_{2P}{}^2(r,z,t)dtdV} = 1 \qquad (22)$$

where V_{in} is the focal volume, V_{out} is the total volume of the sample along the beam path except V_{in}, τ is the pixel dwell time during the imaging, C is the local fluorophore concentration, I is the 2P laser intensity, r is the distance from the optical axis, and z is the axial distance from the sample surface. We assume that the signal and the background share the same fluorescence collection efficiency at the large-area non-descanned detector and the fluorophores are uniformly stained ($C_S = C_B$) throughout the volume. The wavelengths are set as 1000 nm for the two-photon laser and 700 nm for the one-photon laser, both of which lie within the transparent optical window (650 ~1300 nm) of biological tissues. To simplify the calculation, we only consider the ballistic photons for samples whose anisotropy factors are low or moderate, and set the mean free path length as 200 μm, the value for brain tissues of the near IR region [3]. The intensity is shown as

#185684 - $15.00 USD Received 20 Feb 2013; revised 1 Apr 2013; accepted 2 Apr 2013; published 5 Jun 2013

$$I(z)=\frac{P(z)}{A(z)}=\frac{P_0 e^{-z/l_s}}{\omega_0^2\left[1+\left(\frac{(z-z_{focal})}{z_R}\right)^2\right]} \tag{23}$$

where l_s is the mean free path (200 μm), ω_0 is the beam waist at the focus (0.35μm), z_R is the Rayleigh range (0.5μm), and z_{focal} is the depth of the focal plane. Numerical criteria of S/B = 1 determines the 2P imaging-depth limit to be z_{focal} = 1023μm (as shown in Fig. 6), which is very close to the experimental result of ~1 mm on mouse brain tissues [6].

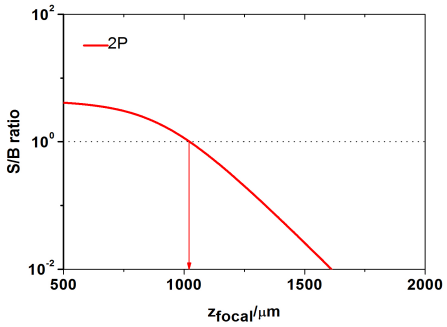

Fig. 6. Numerical estimation of the fundamental imaging-depth limit (where S/B ratio is 1) of the standard 2P microscopy.

We can further calculate the fluorescence photon flux (in the unit of number of photons per microsecond) within the focal volume (V_{in}) and the background volume (V_{out}) respectively. The fluorescence photon flux of the conventional 2P microscopy is given by

$$F_{2P}=\int_V\left(C\varepsilon f_{rep}\right)\left[\sigma_{2P,d}\delta_{2P,d}\left(\frac{I_{2P,ave}\lambda_{2P}}{f_{rep}\delta_{2P}hc}\right)^2\right]d_V. \tag{24}$$

According to Eqs. (8) and (20), the fluorescence photon fluxes of the newly proposed higher-order nonlinear techniques are derived respectively as:

$$F_{enhanced}=\int_V\left(\frac{1}{2}E_tC\varepsilon f_{rep}\right)\left[\sigma_{2P,d}\delta_{2P}\left(\frac{I_{2P,ave}\lambda_{2P}}{f_{rep}\delta_{2P}hc}\right)^2\right]\left[\sigma_{1P,a}\delta_{1P}\left(\frac{I_{1P,ave}\lambda_{1P}}{f_{rep}\delta_{1P}hc}\right)\right]d_V, \tag{25}$$

and

$$F_{3\omega}=\int_V\left(\frac{1}{2}E_tC\varepsilon f_{rep}\right)\left[\sigma_{2P,d}\delta_{2P}\left(\frac{\langle I_{2P,ave}\rangle\lambda_{2P}}{f_{rep}\delta_{2P}hc}\right)^2\right]\left[\sigma_{2P,a}\delta_{2P}\left(\frac{\langle I_{2P,ave}\rangle\lambda_{2P}}{f_{rep}\delta_{2P}hc}\right)^2\right]d_V. \tag{26}$$

Inserting absolute values of the involved parameters (as listed in Table 1), we calculate the signal and background fluorescence photon fluxes, as well as S/B ratio of the conventional two-photon microscopy, two-laser frustrated FRET technique (enhanced) and one-laser frustrated FRET technique (3ω) (Table 1). Our numerical analysis indicates that the two newly proposed frustrated-FRET techniques can dramatically improve the image-contrast at the fundamental imaging depth limit of the standard 2P microscopy. Specifically, the two-laser strategy, which finally creates three-photon effect, increases the signal-to-background

#185684 - $15.00 USD Received 20 Feb 2013; revised 1 Apr 2013; accepted 2 Apr 2013; published 5 Jun 2013

ratio from 1 (normal 2P microscopy) to 46.2; and the one-laser strategy, which creates four-photon effect, enables an improvement of S/B from 1 (normal 2P microscopy) to 294.

Table 1. Comparison of the standard two-photon microscopy, the two-laser frustrated FRET and the one-laser frustrated FRET at the fundamental imaging depth limit of 2P microscopy (z_{focal} = 1023μm) . *

	Two-photon (2P) Microscopy	Two-laser frustrated FRET (3P)	One-laser frustrated FRET (4P)
Signal photon flux [*photon* μs^{-1}]	2.06×10^3	2.42×10^2	1.65×10^1
Background photon flux [*photon* μs^{-1}]	2.06×10^3	5.24×10^0	5.61×10^{-2}
Signal-to-background ratio	1	46.2	294

*The signal and background fluorescence photon fluxes were calculated with a fluorophore concentration of $1.66 \times 10^{-5} M$, a collection efficiency of 0.5, and a FRET efficiency of 80%. The powers were set as 200mW for the 2P laser and 20mW for the 1P laser. Both the two lasers had a repetition rate of 80MHz and the pulse width were 100*fs* and 1*ns* of the 2P and 1P lasers respectively. The two photon cross section of both the donor and acceptor fluorophores were assumed as 100GM and the one photon cross section of the acceptor were assumed as 2×10^{-16}cm^2.

Along with the substantially improved signal-to-background ratio, the super nonlinearity created by frustrated FRET is inevitably associated with a lower fluorescence photon signal than the standard 2P microscopy (Table 1). Hence, the issue of shot noise becomes relevant here. In order for the new techniques to deliver equal signal-to-noise levels as that of the traditional 2P microscopy, prolonged pixel dwell times are needed. For instance, if a 512 pixel × 512 pixel image is taken at 200 Hz with a standard 2P microscopy, which means the pixel dwell time is around 10 μs, 2.06×10^4 photons in total will be collected from a single pixel within the focal volume. To collect a similar number of signal photons, the two-laser technique requires around 85 μs pixel dwell time and the one-laser technique requires around 1250 μs pixel dwell time, which correspond to about 20 Hz and 2 Hz respectively.

2.4 Improvement of the spatial resolution in 3D

In addition to enhancing the signal-to-background contrast deep inside the scattering samples, the super-nonlinearity created by frustrated FRET could also contribute to the enhancement of the spatial resolution. For regular 2P microscopy, the point-spread-function (PSF_{2P}) is the square of the illumination PSF of the 2P excitation laser:

$$PSF_{2P}(x, y, z) = IPSF_{2P}(x, y, z)^2 \tag{27}$$

In the case of two-laser frustrated FRET, the enhanced donor fluorescence signal depends on $I_{2P}{}^2 I_{1P}$. Hence, the $PSF_{enhanced}$ is defined as

$$PSF_{enhanced}(x, y, z) = IPSF_{2P}(x, y, z)^2 IPSF_{1P}(x, y, z) \tag{28}$$

Meanwhile, 3ω harmonic donor fluorescent signal is actually a four-photon signal, which means $PSF_{3\omega}$ is the fourth power of $IPSF_{2P}(x,y,z)$

$$PSF_{2P}(x, y, z) = IPSF_{2P}(x, y, z)^4 \tag{29}$$

$ISPF_{2P}(x,y,z)$ follows a Gaussian-distributed function, and the 1/e widths of lateral and axial profiles for $IPSF_{2P}(x, y, z)^2$ are given by $\omega_{xy} = 0.320\lambda / \sqrt{2} N.A.$ and $\omega_z = 0.532\lambda / \sqrt{2}(n - \sqrt{n^2 - N.A.^2})$, respectively [31].

When using an air-objective with a N.A. = 0.7, the diffraction index (n) as 1, 2P laser wavelength as 1000 nm and 1P laser wavelength as 700 nm, we could plot the point-spread-functions of the donor fluorescence of regular 2P fluorescence signal, enhanced donor

#185684 - $15.00 USD Received 20 Feb 2013; revised 1 Apr 2013; accepted 2 Apr 2013; published 5 Jun 2013

fluorescence signal and the harmonic 3ω signal based on Eqs. (27)-(29). Figure 7 indicates the apparent resolution enhancements by both the frustrated FRET techniques. Compared with the regular 2P microscopy, it is apparent that the one-laser technique (four-photon effect) increases the spatial resolution by a factor of sqrt(2) in all three dimensions. Meanwhile, the two-laser technique (three-photon effect) also improves the resolution by ~1.4 times owing to the relatively shorter wavelength of the 1P laser than that of the 2P laser.

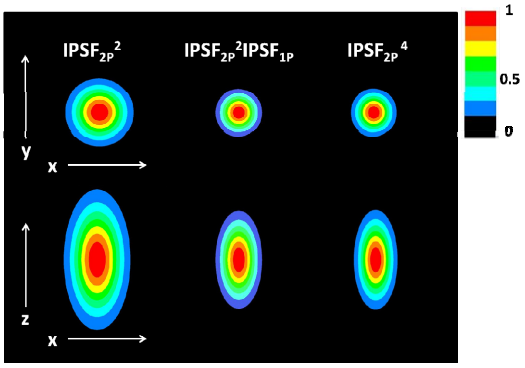

Fig. 7. Both the two-laser and one-laser frustrated FRET techniques can improve the spatial resolution of the regular 2P microscopy in all three dimensions. We assume that the images are taken with an air-objective of N.A. = 0.7, refraction index of 1, and the 2P and 1P laser wavelengths to be 1000 nm and 700 nm, respectively. The color bar linearly depends on the fluorescence intensity: red represents the highest intensity and back represents the lowest intensity.

3. Conclusion

In summary, a new concept of super-nonlinear fluorescence microscopy based on the frustrated FRET effect is proposed to significantly improve image contrast, as well as to enhance the diffraction-limited spatial resolution, of two-photon microscopy deep inside scattering samples. In this article, we described two techniques to generate and detect the higher-order nonlinear signals. In the first approach, we excite the donor and acceptor respectively with two collinearly combined laser beams, and detect the resulting enhanced fluorescence signal. In the second approach, we exploit a single 2P laser beam to excite both donor and acceptor and separate the four-photon signal through harmonic demodulation. Each of these two techniques has its own advantages. The two-laser method allows more efficient and flexible excitation arrangement and hence has a wider range of applicable FRET probes; while the one-laser method requires a relatively simple experimental apparatus. Moreover, by prolonging the collection dwell time accordingly, a signal-to-noise level similar to that of conventional 2P microscopy can be achieved.

Finally, the current approach can be compared with the recently developed deep-imaging methods using photo-activatable fluorophores [32–34]. Both frustrated FRET techniques and mutiphoton activation and imaging of photo-activatable fluorophores represent molecule-based (rather than wave-based) strategies of harnessing special imaging probes with inherent nonlinear response. Owing to the faster temporal response of energy transfer process over chemical bond breaking required in photo-activatable fluorophores, the frustrated FRET techniques should be advantageous in terms of imaging speed especially in *in vivo* applications.

Acknowledgments

We thank L. Zhang, X. Zhu, L. Brus, R. Yuste, D. Peterka, V. Cornish and M. Jimenez for helpful discussions. W.M. acknowledges support from Kavli Institute for Brain Science and RISE program of Columbia University.

#185684 - $15.00 USD Received 20 Feb 2013; revised 1 Apr 2013; accepted 2 Apr 2013; published 5 Jun 2013